chemistry proceedings

MDPI

Proceeding Paper

Design, Development and Insilico Study of Pyrazoline Based Mycobactin Analogs as Anti-Tubercular Agents †

Gourav Rakshit [1], Sheikh Murtuja [2] and Venkatesan Jayaprakash [3,*]

[1] Department of Pharmaceutical Sciences and Technology, Birla Institute of Technology, Mesra, Ranchi 835215, Jharkhand, India; gouravr16@gmail.com
[2] Department of Pharmaceutical Sciences and Technology, Birla Institute of Technology, Mesra, Ranchi 835215, Jharkhand, India; murtazasheikh09@gmail.com
[3] Department of Pharmaceutical Sciences and Technology, Birla Institute of Technology, Mesra, Ranchi 835215, Jharkhand, India
* Correspondence: drvenkatesanj@gmail.com
† Presented at The 25th International Electronic Conference on Synthetic Organic Chemistry.

Abstract: The pathogenicity and virulence of Mycobacterium tuberculosis has further potentiated its infectiousness thereby making it a killer disease as evident from the WHO database. Eradicating the TB epidemic by 2030 is amongst the major health targets of the United Nations Sustainable Development Goals (SDGs). The increase in multidrug-resistant TB (MDR-TB) cases has challenged and prompted the scientific community to develop novel chemotherapeutic agents with novel mechanism of action. This can be achieved by the concept of "conditionally essential target" (CET)-based drug design. The research pertaining to Mycobactin biosynthesis pathway (MBP) relating to iron acquisition is at nascent stage and serves as a promising endogenous target for novel lead compounds discovery (non-specific MBP inhibitors). In continuation to our previous research work reported by Stirret et al., 2008 and Ferreras et al., 2011; here we further aim to explore the structural diversity of the previously identified active molecules which could lead to the discovery of a more potent analog. Eventually we designed a small library of mycobactin analogs retaining the basic scaffold as diaryl-substituted pyrazoline (DAP) and tested their insilico stability by molecular docking (AutoDock 4.2.6). Docking of the designed molecules was performed in the active site of MbtA receptor (by analogy with the related structure PDB: 1MDB) to evaluate the binding modes and inhibitory profile. The lowest energy conformation of each docked ligand was analyzed in BIOVIA Discovery Studio Visualizer. Docking result identified GM08 and GM09 as potent inhibitors and thus could serve as good lead. The ADMET profile also revealed satisfactory results. Further what remains to be seen is the stability of the molecule employing MD simulation and intracellular activity.

Keywords: tuberculosis drug discovery; target-based screening; mycobactins; siderophores; pyrazoline; molecular docking

Citation: Rakshit, G.; Murtuja, S.; Jayaprakash, V. Design, Development and Insilico Study of Pyrazoline Based Mycobactin Analogs as Anti-tubercular Agents. *Chem. Proc.* **2021**, *3*, x. https://doi.org/10.3390/xxxxx

Published: 15 November 2021

1. Introduction

Tuberculosis (TB) is a contagious/infectious diseases transmitted through the air that is caused by the fatal pathogen/bacillus Mycobacterium tuberculosis (Mtb). It has been afflicting humans for ages and is now causing a global health crisis [1]. According to a report released by the World Health Organization (WHO) in 2020, tuberculosis caused around 1.4 million fatalities and over 10 million people were ill with the disease in 2019, signifying a devastating influence on global mortality and morbidity rates [2]. As of today, the WHO believes that one out of every four people has a confirmed tuberculosis infection. MDR TB is a growing pandemic, and the emergence of extended drug-resistant tuberculosis (XDR tuberculosis) offers a new global hazard because it is likely incurable

with current medicines. The United Nations Sustainable Development Goals (SDGs) include a health goal of ending the tuberculosis epidemic by 2030 [3]. To tackle the TB pandemic, innovative treatment medicines with novel modes of action are urgently needed.

This can be achieved by employing the concept of "conditionally essential target" (CET)-based drug design. M. tuberculosis needs iron to colonise and proliferate, as well as to maintain its metabolic machinery [4]. In human serum and bodily fluids, free iron is severely restricted/significantly low (about 10^{-24} M). When faced with a lack of iron in the host, mycobacteria re-uptake tiny molecules known as mycobactins (mycobacterial siderophores/iron chelators) to chelate and ingest this critical trace element from the host iron-binding proteins [5]. The mycobactin production pathway has long been regarded as a promising source of anti-tubercular targets for the creation of new probes. Mycobactin T is highly lipophilic and stays attached to mycobacteria's cell wall, whereas carboxymycobactin, which is more polar due to its short carboxylic acid side chain, is released into the extracellular media by the pathogen to chelate the valuable iron element. The main structures of mycobactins are made up of a 2-hydroxyphenyloxazolidine moiety coupled to an acylated -N-hydroxylysine residue esterified with a 3-hydroxybutyric acid at the -carboxyl. The latter forms an amide bond with a second -N-hydroxylysine, which is then cyclised to provide a lactam (seven membered) [6]. Following the annotation of the M. tuberculosis genome sequence [7], a ten-gene locus (mbtA-J) encoding a non-ribosomal peptide synthetase-polyketide synthase (NRPS-PKS) system was shown to be important for the synthesis of the mycobactin peptide core. MbtA, an aryl-adenylating enzyme, catalyses the first two steps of mycobactin biosynthesis. MbtA activates salicylic acid (adenylation step) by producing Sal-AMP, which is subsequently loaded (acylation step) onto MtbB's phosphopantetheinylation domain, which is also part of the NRPS-PKS cluster [8]. MbtA has no human homologues and has been chemically verified as a target for the development of novel anti-TB agents [9]. M. tuberculosis mutants that are unable to manufacture mycobactins or import these siderophores with chelated iron have been demonstrated to have reduced virulence and proliferation in the lungs and macrophages in vitro and in vivo. Furthermore, nucleoside antibiotics that selectively block MbtA enzymatic activity, such as 5′-O-[N-(salicyl)sulfamoyl)adenosine (Sal-AMS), successfully stopped M. tuberculosis growth and pathogenicity [10]. Taken together, our findings suggest that drugs targeting the mycobactin production pathway would be effective in the treatment of tuberculosis [11].

Stirrett et al. [12] generated a library of small compounds with structural similarities to the mycobactins framework and assessed them against Mtb in 2008, putting the concept of (CET)-based drug design into effect. The 3,5-diaryl-1-carbothioamide-pyrazoline motif, which resembled the hydroxyphenyl-oxazoline unit of the mycobactin and carboxymycobactin siderophores, served as their basic structural scaffold. The compounds were tested for their capacity to suppress Mtb growth in both iron-deficient and iron-rich environments, as well as their ability to block a salicylation enzyme targeted by Sal-AMS. In iron-depleted circumstances, the bactericidal compound (1) had the highest antitubercular activity in the series, with IC_{50} and MIC_{90} values of 8 and 21 M, respectively. Analog 1 had no cytotoxicity against HeLa cells (CD_{50} = 398 M), and it was inactive against Mtb (MIC_{90} = 333 M) in iron-rich conditions GASTD + Fe, showing its involvement in mycobactin system functions, with a remarkable selectivity index (SI_{Mtb} = $IC_{50GASTD}/IC_{50GAST}$) value of 15. Analog 1's structure proved to be a suitable platform for lead design against CETs as well as research into the mycobactin synthesis pathway

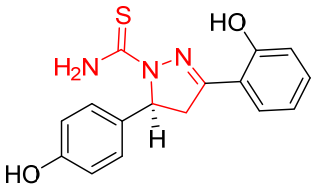

Compound 1

Ferreras et al. [13] created a library of mycobactin analogues including diaryl-substituted pyrazoline (DAP) in 2011 as a follow-up to their previous work. Mtb and Yersinia pestis were tested using DAP derivatives. Compounds 2 and 3 were the most effective against Mtb (IC_{50} = 47 M, MIC = 16 M) among the active DAP derivatives. However, the majority of active compounds had anti-tubercular activity in both iron-depleted (GAST) and iron-replete (GAST + Fe) media, implying that the compounds' targets are linked to mycobacterial activities that are important in both low and high iron environments.

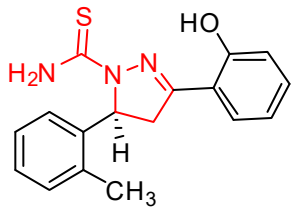

Compound 2

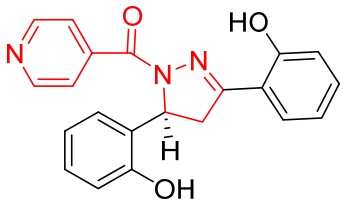

Compound 3

In line with these previous researches, the goal of this work was to identify novel anti-tubercular drugs with a high affinity for MbtA, the adenylating enzyme that catalyses the first step in mycobactin production and is only expressed by mycobacteria. In this regard, we attempted to design a library of 12 compounds by altering the pyrazoline moiety (depicted in red color) of Ferreras et al.'s reported potent molecules (2 and 3) and modified R and R_1 positions respectively. The designed molecules along with their structures are presented in Table 1.

Table 1. Tabular representation of the designed molecules.

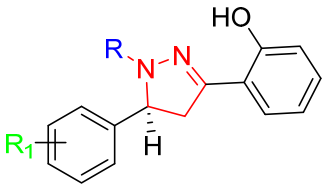

Sl. No.	Code	R	R_1
01	**GM01**	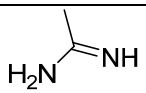	2-CH_3
02	**GM02**	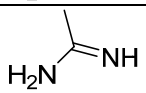	3-CH_3
03	**GM03**	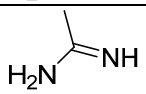	4-CH_3
04	**GM04**	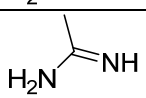	2-OCH_3
05	**GM05**	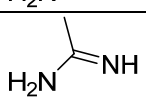	3-OCH_3

06	**GM06**	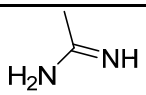	4-OCH_3
07	**GM07**	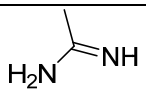	2-Cl
08	**GM08**	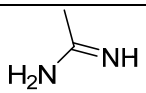	3-Cl
09	**GM09**	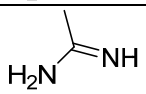	4-Cl
10	**GM10**	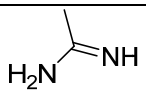	2-OH
11	**GM11**	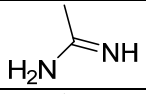	3-OH
12	**GM12**	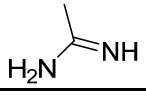	4-OH

To this end, a 12 member library of designed molecules was tested insilico to test the ability to bind to MbtA. These molecules were docked into the active site of the MbtA crystal structure. The top score molecules were taken up for ADME and toxicity studies.

2. Materials and Methods

2.1. Hardware and Software Employed

Docking simulations of current study was done using an HP workstation equipped with Windows 8 single language (64 bit operating system), Intel (R) Core™ i3-3110M CPU @ 2.40 GHz processor system, installed memory (RAM) of 4GB, the hard disk drive of 1TB. Software used was autodock-4.2.6 program for the docking purpose [14], Chemdraw 19.0 (Perkin-Elmer) for sketching and preparation of ligand. Visualizations were done using UCSF Chimera 1.13.1 [15]. BIOVIA Discovery Studio Visualizer program was used for the generation of 2D ligand-protein interaction diagrams [16].

2.2. Docking Simulations

2.2.1. Protein Structure Preparation

The crystal structure of Gene: mbtA consisting of Protein Salicyl-AMP ligase/salicyl-S-ArCP synthetase with UniProt ID: P71716 was selected for the study. The 3D X-ray crystallographic structure/PDB file was obtained from AlphaFold Protein Structure Database. The protein.pdb file was opened in Autodock Tools (ADT), the solvent and ions were removed and the resulting structure was saved as a pdbqt file for use in Autodock.

2.2.2. Ligand Preparation

The designed small molecule ligands were prepared by sketching the 2D structures in ChemDraw 19.1. The 2D representations were converted into 3D structures using Chem3D 19.1 and energy minimized using the integrated MM2 module with default settings. The final stabilized structures were saved in .pdb format for protein-ligand docking.

2.2.3. Protein-Ligand Docking Simulations

The Autodock-4.2.6 program (ADP) was used for all molecular docking studies. The docking algorithm used was the Lamarckian Genetic Algorithm. ADP tools were used to prepare the protein and ligands. The active site was found using UCSF Chimera 1.13.1, and a binding site box (grid box) that was 60 × 60 × 60 in the x, y, and z dimensions was

centered on the nucleotide binding pocket (by analogy with the homologous structure PDB Ref: 1MDB). The default values for all other options were used, i.e., the population size was 150 and the number of Genetic Algorithm (GA) runs was 50. The maximum number of evaluations was 2,500,000. The final procedure involved the running of the auto grid and auto dock. Auto grid-4.2 was used for generating map files and Autodock-4.2 was used for running molecular docking of each ligand on respective protein. From the results file (.dlg), the lowest energy conformation of each docked ligand was retrieved. All docking data were evaluated, and visualizations of various structures were done using Autodock-4.2.

2.3. ADME Prediction

The ADME (absorption, distribution, metabolism, and excretion) of the molecule under investigation, which could be employed as a future lead molecule for drug development, is an important factor in predicting its pharmacodynamics. SWISSADME is a web server built and maintained by the Swiss Institute of Bioinformatics' (SIB) molecular modelling group (https://www.swissadme.ch) [17]. Already created structures of ligands/molecules were uploaded individually in the Marvin JS portion of the website http://swissadme.ch/index.php to compute ADME parameters. Structures were automatically translated to SMILES format, and the server predicted ADME. The collected results were stored for further investigation.

2.4. Toxicity Prediction

Toxicology prediction is a crucial feature of all compounds. PkCSM is a web server database that allows users to analyze molecules by either sketching them graphically or providing them in SMILES format [18]. The toxicity information on the web server database includes AMES toxicity, maximum tolerated dose, hepatotoxicity, skin sensitivity, and hERG I and II inhibitors. After logging into the website, the SMILES of the top-scoring compounds after docking were searched and submitted, and toxicity was chosen in prediction mode.

3. Results

3.1. Docking Simulation Studies

The docking investigation of all the ligands with MbtA protein showed favorable binding energies and inhibition constants. Top score compounds namely **GM08 (−9.90, 55.54 nM)**, **GM09 (−9.83, 62.70 nM)**, **GM02 (−9.72, 74.65 nM)**, and **GM03 (−9.64, 85.71 nM)** indicated a high affinity for the binding pocket and had high negative binding energies. The binding energies/docking scores and inhibition constants of all molecules are given in Table 2.

Table 2. Details of docking-based parameters of designed compounds in the binding pocket of target MbtA protein.

Sl No.	Code	Dock Score	Inhibition Constant
01	**GM01**	−9.23	171.39 nM
02	**GM02**	−9.72	74.65 nM
03	**GM03**	−9.64	85.71 nM
04	**GM04**	−9.19	182.87 nM
05	**GM05**	−9.41	126.09 nM
06	**GM06**	−9.49	110.58 nM
07	**GM07**	−9.32	148.14 nM
08	**GM08**	−9.90	55.54 nM
09	**GM09**	−9.83	62.70 nM
10	**GM10**	−8.58	510.97 nM

11	**GM11**	−9.04	235.3 nM
12	**GM12**	−8.86	317.69 nM

The binding conformations of the top score four compounds in the active site/binding pocket involved H-bond interactions with residues of the interacting protein. The details of the residues involved in bonding with ligands i.e., H-bond interactions residues are given in Table 3 and the docking images are shown in Figures 1–4.

Table 3. Details of top score identified compounds showing H-bond interacting residues in the binding pocket of MbtA.

Sl No.	Ligand Code	H-Bond Residues
1.	**GM08**	Gly460, Thr462, Ala356
2.	**GM09**	Gly460, Thr462, Ala356
3.	**GM02**	Gly460, Thr462, Ala356
4.	**GM03**	Gly460, Thr462, Ala356

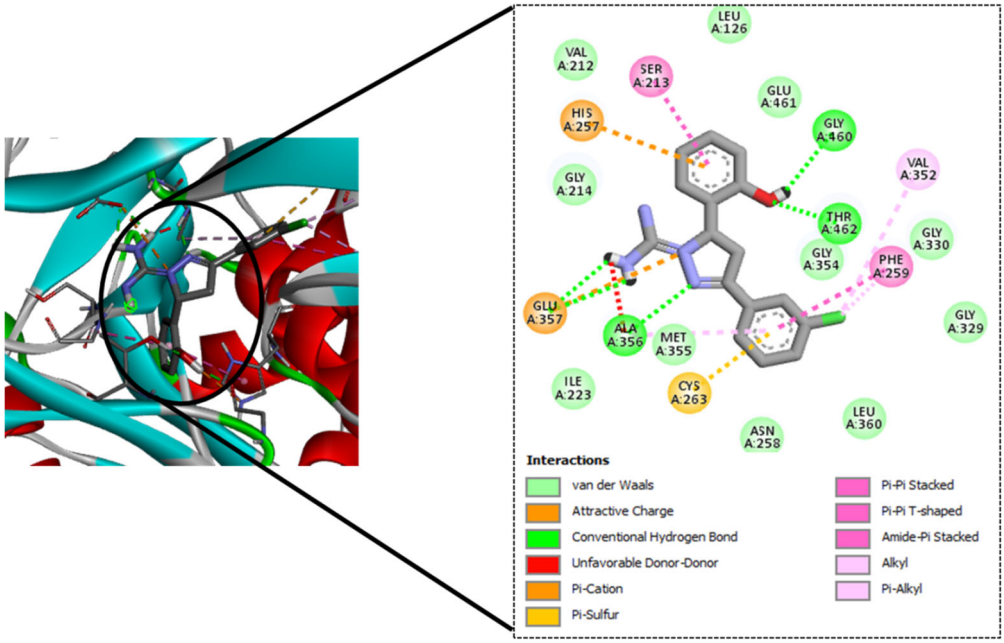

Figure 1. Docking interaction of GM08 in the binding pocket of MbtA showing three hydrogen bonds.

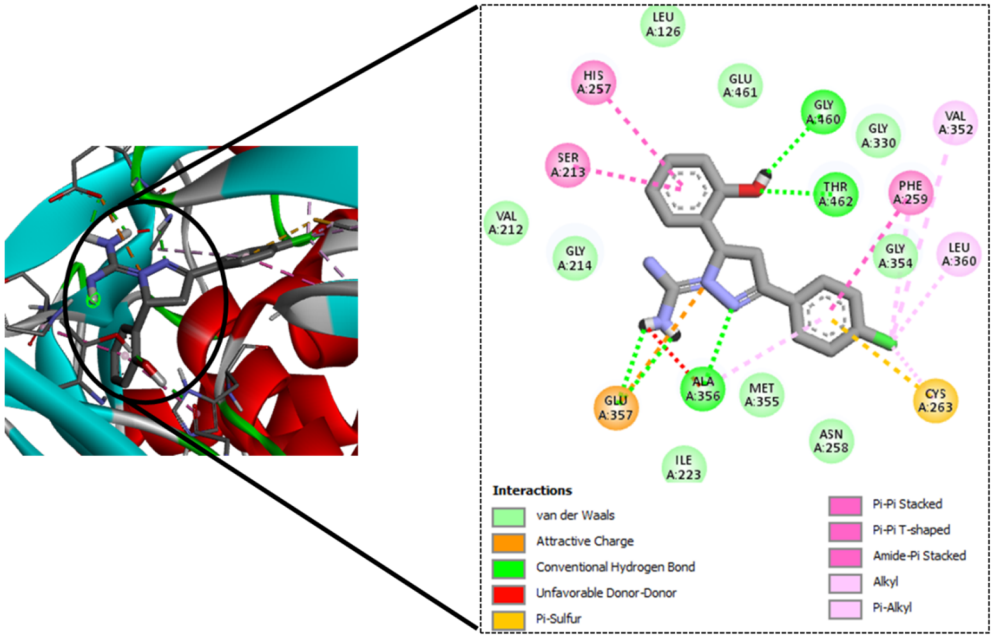

Figure 2. Docking interaction of GM09 in the binding pocket of MbtA showing three hydrogen bonds.

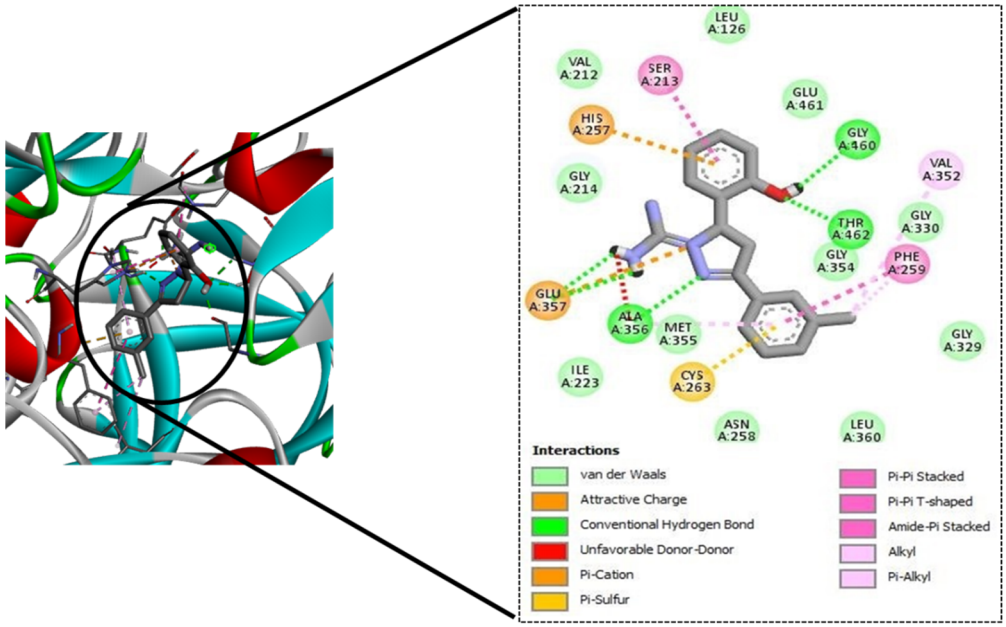

Figure 3. Docking interaction of GM02 in the binding pocket of MbtA showing three hydrogen bonds.

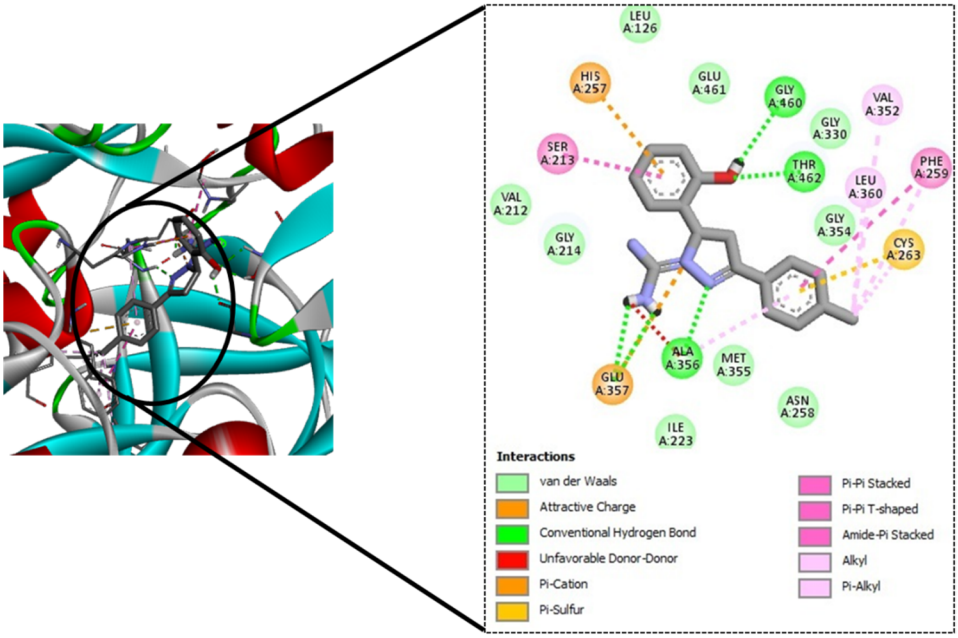

Figure 4. Docking interaction of GM03 in the binding pocket of MbtA showing three hydrogen bonds.

3.2. ADME Prediction

3.2.1. Results of Drug-Likeness, Bioavailability, Synthetic Feasibility and Alerts for PAINS & Brenk Filters

The likelihood of a compound becoming an oral drug in terms of bioavailability is referred to as drug-likeness. The drug-likeness of our twelve query compounds was calculated using five distinct filters, as shown in Table 4. The results showed that all of the compounds tested (**GM08**, **GM09**, **GM02**, and **GM03**) had an excellent drug-likeness score and no violations of drug-likeness rules, as well as a good lead-likeness score. To identify the possible uncertain fragments that result in false-positive biological output, the PAINS and Brenk methods were used. As a result of the inclusion of fragments, all compounds were found to be in violation. Along with the synthetic accessibility evaluation, the lead likeness for the compounds was computed. Because their scores were in the range of 3.52–3.65, the obtained data suggested that these four compounds might be easily synthesised. The Abbot Bioavailability score predicts whether a chemical has 10% oral bioavailability (in rats) or a measurable Caco-2 cell line permeability assay, and is defined by a feasibility value of 11 percent, 17 percent, 56 percent, or 85 percent. All the compounds were predicted at 56 percent, indicating good bioavailability.

Table 4. Tabular representation of different drug-likeness rules, bioavailability, lead-likeness, synthetic accessibility, and alerts for PAINS and Brenk.

Sl No.	Compound Code	Drug-Likeness Rules						Alerts		Lead Likeness	Synthetic Accessibility
		Lipinski (Pfizer)	Ghose (Amgen)	Veber (GSK)	Egan (Pharmacia)	Muege (Bayer)	Bioavailability Score	PAINS	Brenk		
1.	**GM08**	Yes	Yes	Yes	Yes	Yes	0.55	1	2	Yes	3.52
2.	**GM09**	Yes	Yes	Yes	Yes	Yes	0.55	1	2	Yes	3.52
3.	**GM02**	Yes	Yes	Yes	Yes	Yes	0.55	1	2	Yes	3.65
4.	**GM03**	Yes	Yes	Yes	Yes	Yes	0.55	1	2	Yes	3.63

3.2.2. In-Silico Evaluation of Pharmacokinetics Compliance

The success of a drug's trip throughout the body is measured in terms of ADME (absorption, distribution, metabolism, and elimination). By computing the different physico-

chemical and bio-pharmaceutical features, the ADME parameters for the substances under research, GM08, GM09, GM02, and GM03, were derived. The molar refractivity, which accounts for the overall polarity of the molecules, was 95.36 (GM08 and GM09) and 95.31 (GM02 and GM03) in the acceptable range (30–140). For all compounds, the topological polar surface area (TPSA) was 85.702 Å^2. These findings indicate that the molecules are unable to pass the blood-brain barrier (BBB). The capacity of a molecule to dissolve itself in a lipophilic medium is referred to as solubility class lipophilicity, and it correlates to various representations of drug properties that affect ADMET, such as permeability, absorption, distribution, metabolism, excretion, solubility, plasma protein binding, and toxicity. The iLOGP and SILICOS-IT results showed that the iLOGP values of the four molecules under investigation (GM08 = 2.05, GM09 = 2.02, GM02 = 2.02, and GM03 = 2.10) were within the acceptable range (−0.4 to +5.6), while the SILICOS-IT values (GM08 = 2.57, GM09 = 2.57, GM02 = 2.44, and GM03 = 2.44) were in the most favourable range. These compounds had a high rate of intestinal absorption. The solubility of a medicine in water is an essential factor in its absorption and distribution. The molecule's solubility in water at 25°C is represented by log S calculations. The computed log S values through the ESOL model should not exceed 6 for appropriate solubility. The log S value for GM08 and GM09 was −3.57, whereas the value for GM02 and GM03 was −3.28, indicating low solubility. The data suggests that these compounds have a good balance of permeability and solubility, and that they would have acceptable bioavailability when given orally. For all compounds, predicted GI absorption was high. Permeability predictions aid in the comprehension of ADMET and cell-based bioassay results. The permeability over human skin for GM08 and GM09 was −6.45 cm/s, and −6.51 cm/s for GM02 and GM03, all of which were within acceptable limits. As previously stated, none of these substances demonstrated the ability to penetrate the BBB. Drug-drug interactions and drug bioavailability are sometimes caused by metabolism. Drug-metabolizing enzymes can only bind to the free form of the drug. The interaction of our main compounds with cytochrome P450 enzymes (CYPs), the most well-known class of metabolising enzymes, is critical for understanding their metabolic behaviour. All four compounds were tested for their ability to inhibit CYPs (CYPs of human liver microsomes (HLM)). Detailed analyses are mentioned in Table 5.

Table 5. Details of in-silico ADME Profile of four selected compounds using Swiss ADME online server.

			GM08	GM09	GM02	GM03
ADMET PROFILE	Physiochemical parameters	Formula	$C_{16}H_{15}ClN_4O$	$C_{16}H_{15}ClN_4O$	$C_{17}H_{18}N_4O$	$C_{17}H_{18}N_4O$
		Molecular weight	314.77 g/mol	314.77 g/mol	294.35 g/mol	294.35 g/mol
		Mol. refractivity	95.36	95.36	95.31	95.31
		TPSA	85.70 Å^2	85.70 Å^2	85.70 Å^2	85.70 Å^2
	Lipophilicity	ILOGP	2.05	2.02	2.02	2.10
		SILICOS-IT	2.57	2.57	2.44	2.44
	Water Solubility	Log S (ESOL), Class	−3.57	−3.57	−3.28	−3.28
		Log S (Ali), Class	−3.93	−3.93	−3.66	−3.66
		SILICOS-IT, Class	−4.64	−4.64	−4.42	−4.42
	Pharmacokinetics	GI absorption	High	High	High	High
		BBB permeant	No	No	No	No
		Log K_P (skin perm.)	−6.45 cm/s	−6.45 cm/s	−6.51 cm/s	−6.51 cm/s
		CYP1A2	Yes	Yes	No	No

CYP2C19	No	No	No	No
CYP2C9	No	No	No	No
CYP2D6	No	No	No	No
CYP3A4	No	No	No	No

3.3. Toxicity Prediction

The toxicity of the identified compounds **GM08**, **GM09**, **GM02**, and **GM03** was investigated in-silico. The maximum tolerated dosage (human) range for all of the molecules was found to be in between −0.127 and −0.199 Log mg/kg/day. No hERGI (human Ether-a-go-go-Related Gene) inhibition was found, however all drugs inhibited hERG II. The results revealed no intracellular buildup of phospholipids (known to cause QT prolongation, myopathy, hepatotoxicity reaction, nephrotoxicity, and pulmonary dysfunction). The software predicted no hepatotoxicity and cutaneous hypersensitivity in any of the compounds. All the predicted toxicity results of **GM08**, **GM09**, **GM02**, and **GM03** molecules are mentioned in Table 6.

Table 6. Tabular representation data of predicted toxicity of top four compounds.

Model Name	Units	GM08	GM09	GM02	GM03
AMES toxicity	Yes/No	Yes	No	Yes	Yes
Max. tolerated dose (human)	Log mg/kg/day	−0.127	−0.177	−0.15	−0.199
hERG I inhibitor	Yes/No	No	No	No	No
hERG II inhibitor	Yes/No	Yes	Yes	Yes	Yes
Oral Rat Chronic Toxicity (LD50)	Mol/kg	3.272	3.273	3.257	3.258
Oral Rat Chronic Toxicity	Log mg/kg_bw/day	1.498	1.566	1.415	1.519
Hepatotoxicity	Yes/No	No	No	No	No
Skin Sensitisation	Yes/No	No	No	No	No
T. Pyriformis toxicity	Log ug/L	0.264	0.274	0.262	0.271
Minnow toxicity	Log mM	1.143	1.396	1.361	1.614

4. Conclusions

TB remains a substantial health burden in underdeveloped nations, despite significant progress in clinical drug candidate development for TB treatment during the last 10–15 years. The search for therapeutic candidates that inhibit novel targets is still a hot topic in science. Studies aimed at gaining a better knowledge of Mtb biology have yielded some results, including the discovery of new therapeutic targets. It has been established that mycobacterial virulence and survival in the host are directly affected by impairments in mycobactin production and iron uptake. The rational design of MbtI and MbtA inhibitors based on structure has so far yielded encouraging results. To this goal, we used the notion of CET-based drug design to find M. tuberculosis inhibitors that can bind to a well-defined target, namely MbtA. The tubercular enzyme MbtA, a newly discovered TB target that catalyses the initial two-step reaction of mycobactin production, was found to highly interact with our top four designed compounds (**GM08**, **GM09**, **GM02**, and **GM03**). They also showed acceptable pharmacokinetic profile and a nominal toxicity profile. Further based on docking score and predicted pharmacokinetic profile it could be concluded that **GM08** and **GM09** could serve as good leads for future optimization. Further; exploring intrinsic interactions between potential drugs and their potential therapeutics could open the way for unique and modern antibiotic discovery methodologies to be developed and implemented.

Funding: This research received no funding.

Acknowledgments: We would like to express our sincere gratitude to our Department of Pharmaceutical Sciences and Technology, Birla Institute of Technology, Mesra, Ranchi for providing the necessary software and supporting this research work.

Conflicts of Interest: The authors declare no conflict of interest

References

1. Daniel, T.M.; Bates, J.H.; Downes, K.A. History of tuberculosis. *Tuberc. Pathog. Prot. Control* **1994**, 13–24, doi:10.1128/9781555818357.ch2.
2. World Health Organization. Global Task Force on TB Impact Measurement. 2019. Available online: https://www.who.int/groups/global-task-force-on-tb-impact-measurement (accessed on).
3. World Health Organization. Tuberculosis; Key facts. 2021. Available online: https://www.who.int/news-room/fact-sheets/detail/tuberculosis (accessed on).
4. Shyam, M.; Shilkar, D.; Verma, H.; Dev, A.; Sinha, B.N.; Brucoli, F.; Bhakta, S.; Jayaprakash, V. The Mycobactin biosynthesis pathway: A prospective therapeutic target in the battle against tuberculosis. *J. Med. Chem.* **2020**, *64*, 71–100.
5. Lamb, A.L. Breaking a pathogen's iron will: Inhibiting siderophore production as an antimicrobial strategy. *Biochim. Biophys. Acta (BBA)-Proteins Proteomics* **2015**, *1854*, 1054–1070, .
6. de Voss, J.J.; Rutter, K.; Schroeder, B.G.; Barry, C.E., III. Iron acquisition and metabolism by mycobacteria. *J. Bacteriol.* **1999**, *181*, 4443–4451, .
7. Cole, S.T.; Brosch, R.; Parkhill, J.; Garnier, T.; Churcher, C.; Harris, D.; Gordon, S.V.; Eiglmeier, K.; Gas, S.; Barry, C.E., III; et al. Deciphering the biology of Mycobacterium tuberculosis from the complete genome sequence. *Nature* **1998**, *396*, 190.
8. de Voss, J.J.; Rutter, K.; Schroeder, B.G.; Su, H.; Zhu, Y.; Barry, C.E. The salicylate-derived mycobactin siderophores of Mycobacterium tuberculosis are essential for growth in macrophages. *Proc. Natl. Acad. Sci. USA* **2000**, *97*, 1252–1257, .
9. Lun, S.; Guo, H.; Adamson, J.; Cisar, J.S.; Davis, T.D.; Chavadi, S.S.; Warren, J.D.; Quadri, L.E.N.; Tan, D.S.; Bishai, W.R. Pharmacokinetic and in vivo efficacy studies of the mycobactin biosynthesis inhibitor salicyl-AMS in mice. *Antimicrob. Agents Chemother.* **2013**, *57*, 5138–5140, .
10. Reddy, P.V.; Puri, R.V.; Chauhan, P.; Kar, R.; Rohilla, A.; Khera, A.; Tyagi, A.K. Disruption of mycobactin biosynthesis leads to attenuation of Mycobacterium tuberculosis for growth and virulence. *J. Infect. Dis.* **2013**, *208*, 1255–1265.
11. Duckworth, B.P.; Nelson, K.M.; Aldrich, C.C. Adenylating enzymes in Mycobacterium tuberculosis as drug targets. *Curr. Top. Med. Chem.* **2012**, *12*, 766–796.
12. Stirrett, K.L.; Ferreras, J.A.; Jayaprakash, V.; Sinha, B.N.; Ren, T.; Quadri, L.E.N. Small molecules with structural similarities to siderophores as novel antimicrobials against Mycobacterium tuberculosis and Yersinia pestis. *Bioorg. Med. Chem. Lett.* **2008**, *18*, 2662–2668, .
13. Ferreras, J.A.; Gupta, A.; Amin, N.D.; Basu, A.; Sinha, B.N.; Worgall, S.; Jayaprakash, V.; Quadri, L.E.N. Chemical scaffolds with structural similarities to siderophores of nonribosomal peptide–polyketide origin as novel antimicrobials against Mycobacterium tuberculosis and Yersinia pestis. *Bioorg. Med. Chem. Lett.* **2011**, *21*, 6533–6537.
14. Morris, G.M.; Huey, R.; Lindstrom, W.; Sanner, M.F.; Belew, R.K.; Goodsell, D.S.; Olson, A.J. AutoDock4 and AutoDockTools4: Automated docking with selective receptor flexibility. *J. Comput. Chem.* **2009**, *30*, 2785–2791.
15. Pettersen, E.F.; Goddard, T.D.; Huang, C.C.; Couch, G.S.; Greenblatt, D.M.; Meng, E.C.; Ferrin, T.E. UCSF Chimera—a visualization system for exploratory research and analysis. *J. Comput. Chem.* **2004**, *25*, 1605–1612.
16. Dassault Systèmes. *BIOVIA Discovery Studio Visualizer*; Dassault Systèmes: San Diego, CA, USA, 2021.
17. Daina, A.; Michielin, O.; Zoete, V. SwissADME: a free web tool to evaluate pharmacokinetics, drug-likeness and medicinal chemistry friendliness of small molecules. *Sci. Rep.* **2017**, *7*, 1–13.
18. Pires, D.E.V.; Blundell, T.L.; Ascher, D.B. pkCSM: Predicting small-molecule pharmacokinetic and toxicity properties using graph-based signatures. *J. Med. Chem.* **2015**, *58*, 4066–4072, doi: 10.1021/acs.jmedchem.5b00104.